Nuclear Materials and Energy 12 (2017) 582–587

Contents lists available at ScienceDirect

Nuclear Materials and Energy

journal homepage: www.elsevier.com/locate/nme

# Studies of dust from JET with the ITER-Like Wall: Composition and internal structure

E. Fortuna-Zaleśna[a,*], J. Grzonka[a,b], M. Rubel[c], A. Garcia-Carrasco[c], A. Widdowson[d], A. Baron-Wiechec[d], L. Ciupiński[a], JET Contributors[e,1]

[a] Faculty of Materials Science and Engineering, Warsaw University of Technology, 02-507 Warsaw, Poland
[b] Institute of Electronic Materials Technology, 01-919 Warsaw Poland
[c] Department of Fusion Plasma Physics, Royal Institute of Technology (KTH), 100 44 Stockholm, Sweden
[d] CCFE, Culham Science Centre, Abingdon, OX14 3DB, UK
[e] EUROfusion Consortium, JET, Culham Science Centre, Abingdon, OX14 3DB, UK

ARTICLE INFO

*Article history:*
Received 7 July 2016
Revised 3 November 2016
Accepted 26 November 2016
Available online 27 January 2017

*Keywords:*
Dust
JET
ITER-Like Wall
Beryllium
Tungsten
Material mixing

ABSTRACT

Results are presented for the dust survey performed at JET after the second experimental campaign with the ITER-Like Wall: 2013–2014. Samples were collected on adhesive stickers from several different positions in the divertor both on the tiles and on the divertor carrier. Brittle dust-forming deposits on test mirrors from the inner divertor wall were also studied. Comprehensive characterization accomplished by a wide range of high-resolution microscopy techniques, including focused ion beam, has led to the identification of several classes of particles: (i) beryllium flakes originating either from the Be coatings from the inner wall cladding or Be-rich mixed co-deposits resulting from material migration; (ii) beryllium droplets and splashes; (iii) tungsten and nickel-rich (from Inconel) droplets; (iv) mixed material layers with a various content of small (8–200 nm) W-Mo and Ni-based debris. A significant content of nitrogen from plasma edge cooling has been identified in all types of co-deposits. A comparison between particles collected after the first and second experimental campaign is also presented and discussed.



## 1. Introduction

Processes of dust generation and transport have been studied in present-day tokamaks for the last two decades. The main driving forces in research have been related to a whole spectrum of safety aspects and then licensing of a future reactor-class device, e.g. ITER. This has also included the assessment of deposition and dust formation on the reliability of in-vessel diagnostic components, especially metallic first mirrors. Therefore, detailed dust surveys have been carried out regularly in all medium- and small-size tokamaks and in several simulators of plasma-wall interaction (PWI). The bibliography of works performed until year 2010 is in [1], while results of recent examination in several machines are also available: TEXTOR [2,3], Tore Supra [2,4], ASDEX-Upgrade [5,6], FTU [7] and other machines.

Operation of JET with the ITER-Like Wall (JET-ILW) has brought a spectrum of new research aims and results connected to the new wall structure and composition: beryllium in the main chamber and tungsten in the divertor [8–9]. It has created new challenges related to the analysis of materials retrieved from the torus: marker tiles, wall probes [10,11] and dust. The aim in studying dust from JET-ILW is to provide a robust data base for the predition of dust generation in ITER, particularly categories and major formation mechanisms. Though JET-ILW has the best possible proximity to ITER, in PWI studies both similarities and differences in the structure of plasma-facing components (PFC) between two machines are thoroughly taken into account, e.g. solid Be and W components in ITER, while in some areas of JET-ILW tiles with either tungsten or beryllium coatings are used, as detailed in [8].

Dust retrieval was performed by vacuum cleaning during major in-vessel interventions (shut-downs) after two ILW campaigns from 22 out of 24 divertor modules: around 1.4 g after 2011–2012 and 1.8 g after 2013–2014 operation [12], thus corresponding to about 0.06 g $m^{-2}$ and 0.08 g $m^{-2}$ of the divertor surface area, respectively. When scaled to plasma operation time, these amounts were over two orders of magnitude smaller than those retrieved

* Corresponding author.
*E-mail addresses:* efortuna@o2.pl, efortuna@inmat.pw.edu.pl (E. Fortuna-Zaleśna).
[1] *See the Appendix of Romanelli et al Proc. 25th IAEA Fusion Energy Conf., Saint Petersburg, Russia*

http://dx.doi.org/10.1016/j.nme.2016.11.027

**Table 1**
List of studied materials with details on their origin and sampling location given in terms of the S-coordinate.

| Tile / Sample | Region | Sampling location: S-coordinate (mm) |
|---|---|---|
| 0 | Outside deposition zone | 110 |
| 0 | Deposition zone | 137 |
| 1 | Apron (horizontal part of Tile 1) | 210 |
| 3 | Lower part below | 590 |
| 6 | Deposition zone in shadow of Tile 7 | 1415 |
| Under tile 6 | Divertor carrier | n/a |
| Mirror 119 | Inner divertor, first mirror in the cassette | n/a |

after the 2007–2009 campaign in JET with the carbon wall (JET-C) [13]. Besides vacuum cleaning, after the first ILW campaign dust, was also sampled by a carbon sticker from a single location in the inner divertor [14]. A widespread collection was performed after the second campaign.

This paper is focused on detailed studies of material sampled from many points on the divertor tiles and on the test mirrors located in the main chamber. The main goal is to relate the morphology of dust from various locations with the overall deposition pattern and with the operation history. This also includes a comparison of internal structure of co-deposits from the inner divertor after the two campaigns in JET-ILW, in the following called ILW-1 and ILW-2. The emphasis is on particles relevant from the ITER point of view: Be-rich deposits and metal droplets, while debris from W-coated carbon fibre composite (W/CFC) tiles will be only briefly addressed, as not relevant because no such coatings are foreseen for a reactor-class machine.

## 2. Experimental

The study was carried out for samples collected on tiles from the divertor modules which were not vacuum cleaned after the 2013–2014 campaign. Two complete modules equipped with erosion-deposition diagnostics [10] were transferred from the torus to the Beryllium Handling Facility (BeHF). Dust sampling was done manually at several different positions using adhesive carbon pads of 2.54 cm (1 inch) in diameter. This method enables a direct correlation between the location and the type of dust particles. However, the procedure has one disadvantage: only the bottom part and some side surfaces of the collected matter can be examined by optical or scanning electron microscopy (SEM), because the top layer is embedded in the glue of a pad. This problem is partly overcome by using focused ion beam (FIB) technique to obtain cross-sections of particles, but even this approach still prevents direct studies of the top layers. It is also limited to objects not thicker than 20 µm; above that value the quality of results is degraded. The information on the sampling is detailed in Table 1, while the image in Fig. 1 shows the divertor poloidal cross-section.

Dust found under Tile 6 on the frame of the divertor carrier was collected by wiping with a swab and then the matter was transferred to a sticky pad. In addition, brittle and dust-forming co-deposits on a metallic test mirror (First Mirror Test, FMT [15,16]) was examined. The mirror was located in the inner divertor in the shadow of Tile 3. No special dust sampling was required in this case.

The composition, size, surface topography and internal features of dust and deposits were examined using a large set of electron and ion beam methods. The analyses performed at the Warsaw University of Technology comprised: SEM (Hitachi SU 8000) combined with energy-dispersive X-ray spectroscopy (EDX, Thermo Scientific Ultra Dry, type SDD enabling Be analysis), focused ion beam (FIB/SEM, Hitachi NB5000) and scanning transmission electron microscopy (STEM, Aberration Corrected Dedicated STEM Hitachi HD-2700). Depth profiling (Be, C, N, O, W) was determined by time-of-flight heavy ion elastic recoil detection analysis (ToF–ERDA) with a 36 MeV $^{127}I^{8+}$ beam. The method gives good depth resolution of a few nm and it is particularly suited for studying smooth surfaces, e.g. mirrors. The information depth is limited to a few hundreds of micrometers because of a low incidence angle (22°). Global fuel retention studies (i.e. deuterium content analysis) could not be performed on samples collected by sticky pads. Thermal desorption, for obvious reasons, is out of question. However, detailed information on fuel retention in deposits determined by ion beam analysis (IBA) can be found [12].

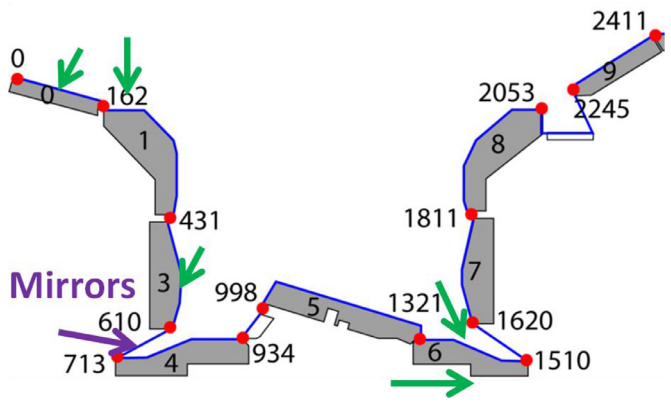


**Fig. 1.** Divertor poloidal cross-section in JET-ILW. Numbers correspond to S-coordinate denoting poloidal length in the divertor. Red dots mark edge point of respective tiles. Green arrows indicate positions of dust sampling, while the position of a cassette with mirrors in the inner divertor is marked with a violet arrow. (For interpretation of the references to colour in this figure legend, the reader is referred to the web version of this article.)

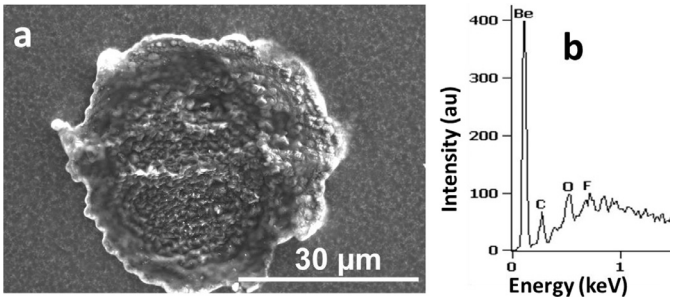


**Fig. 2.** (a) Beryllium flakes from the inner wall cladding on Tile 0 in the area without deposits, SEM SE image and (b) corresponding EDX spectrum.

## 3. Results and discussion

The presentation of dust survey follows the divertor poloidal cross-section starting from the inner divertor Tile 0 which acts as the High Field Gap Closure (HFGC) plate. A comparison of dust after the consecutive campaigns will be made for apron on Tile 1. The description of dust collected from plasma-facing surfaces will be complemented by the characterisation of particles taken from the divertor carrier below Tile 6. Finally, dust-forming deposits on the test mirror will be presented.

### 3.1. Dust on divertor tiles

Tile 0 has two distinct regions: shiny and “blackish” . A sample collected outside the “blackish” deposition zone is characterised by a small density of particles: thin though fairly large (dimensions from 30 µm to 300 µm) flakes rich in beryllium. It is documented by the image of a flake in Fig. 2(a). The corresponding X-ray spec-

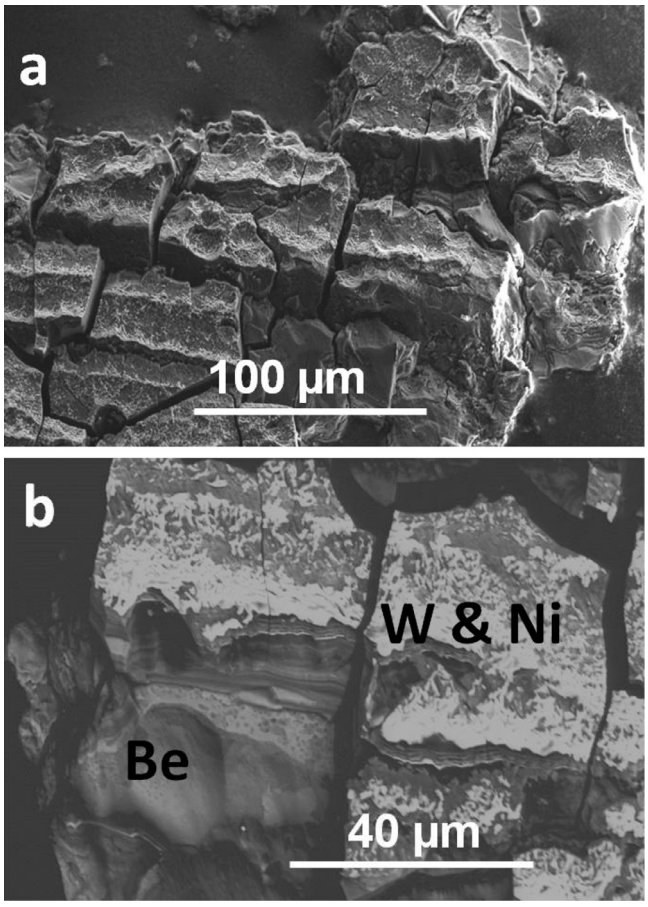


**Fig. 3.** Thick co-deposits collected in the deposition zone of Tile 0 after ILW-2, a) SE mode, b) BSE mode.

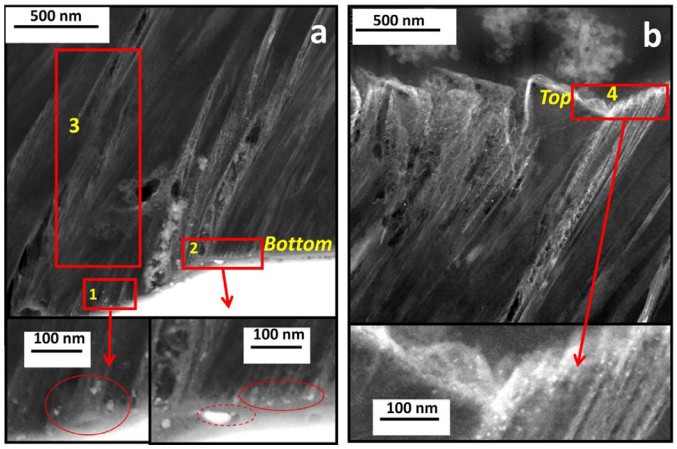


**Fig. 4.** STEM images of: (a) the bottom and (b) top layer of beryllium flake on apron of Tile 1 after the ILW-1 campaign in 2011–2012. In red circles the regions rich in W particles are indicated. (For interpretation of the references to colour in this figure legend, the reader is referred to the web version of this article.)

trum, Fig. 2(b) clearly proves that Be is the major constituent. The structure of the flakes has features of Be coatings from the inner wall cladding tiles, as observed in secondary electron images. The structure of some areas suggests that the material was molten.

Images in Fig. 3 show particles of mixed columnar and stratified structure detached from the deposition zone: thick and cracked Be-based layers. There are regions rich in tungsten and nickel: bright areas in Fig. 3(b) recorded in the backscattered electron (BSE) mode and analysed with EDX. While the presence of tungsten may be attributed to the detachment of underlying W coating on the CFC tile, the presence of nickel can only be related to the deposition of that element eroded from the in-vessel Inconel components: torus wall or a grill of the antenna for ion or electron resonance heating, or from damaged tie rods in Tile 7. The studied region on Tile 0 is known to be the major deposition zone in the divertor with the deposit thickness reaching 50 µm (cumulative after two campaigns) and the deuterium content of up to $1 \times 10^{19}$ cm$^{-2}$ [12].

For Tile 1 the analyses have been concentrated on the apron area which may be perceived as the extension of Tile 0, also from the point of view of deposition: layers up to 20 µm thick [12,17–19]. Dust from the apron was sampled after each campaign. This allows for a meaningful comparison because the operation time was similar in both cases: around 19.5 h including approximately 6.5 h of limiter and 13 h of X-point plasmas. After the first campaign the most important result was the identification of Be dust in the form of droplets and flakes detached from co-deposited layers. The internal structure of such flakes has been recently examined. STEM images in Fig. 4(a) and (b) show, respectively, the bottom and top layer of a 4 µm thick flake formed during ILW-1. Bottom of the layer corresponds to the initial phase of operation, while the top is related to end of the 2011–2012 ILW campaign. A crystalline columnar structure suggests quiescent growth of the deposit. The layer contains also tungsten particles: approximately 10–15 nm in diameter. They are found only locally at the very bottom of the layer: around 10 particles in the area of about $100 \times 100$ nm, Areas 1 and 2 in Fig. 4(a). There are also a few bigger objects (50 nm) in Area 2 which may originate directly from the W-coating on the tile. This statement is justified by the fact that there are no W and any other high- or medium-Z particles in Area 3. This area (and actually the whole image in Fig. 4a) corresponds to the early stage of the layer formation during the L-mode discharges at the beginning of the first ILW campaign: relatively low power and, therefore, low erosion of tungsten from the wall. Significantly increased number of 4–15 nm W particles (hundreds in the area $350 \times 500$ nm) is in the upper part of the layer thus suggesting the increased deposition of W at the final stages of campaign, i.e. period with H-mode operation; it is shown in Fig. 4(b) and detailed for Area 4. The presence of W inclusions is most probably attributed to the erosion of W-coated carbon fibre composite (W/CFC) tiles in the divertor and some places on the main chamber wall. As a consequence, the composition of deposits is clearly correlated with the history of operation: L-mode in the initial phase and a greater input power for H-mode discharges towards the end. Disruptions at high power shots additionally contributed to the generation of tiny metal particles.

Examples of dust collected from the Tile 1 apron after the second campaign with most discharges in the H-mode are in Fig. 5(a)–(d), showing a 200 µm object, EDX spectra from two regions (marked 1 and 2) and STEM images for cross-sections from two different areas of that object. Already an overview BSE image in Fig. 5(a) indicates a complex mix of light and heavy elements. A cross section in Fig. 5(c) recorded in the high-angle-annular dark field (HAADF) mode shows fairly uniform co-deposit composed of low-Z elements (Be, C, O, N) with only one remarkable tungsten layer visible as a bright stripe. Another cross-section, Fig. 5(d), is a sandwich of low-Z (beryllium-carbon) strata and regions with 100–200 nm inclusions of heavy metals (tungsten and nickel) in the low-Z matrix. Tungsten can originate both from the bulk metal (Tile 5) and coated tiles, while nickel must come from Inconel or steel components in the main chamber. It should be stressed that all types of co-deposits after the 2013–2014 campaign (dominated either by light or heavy elements) contain significant amounts of

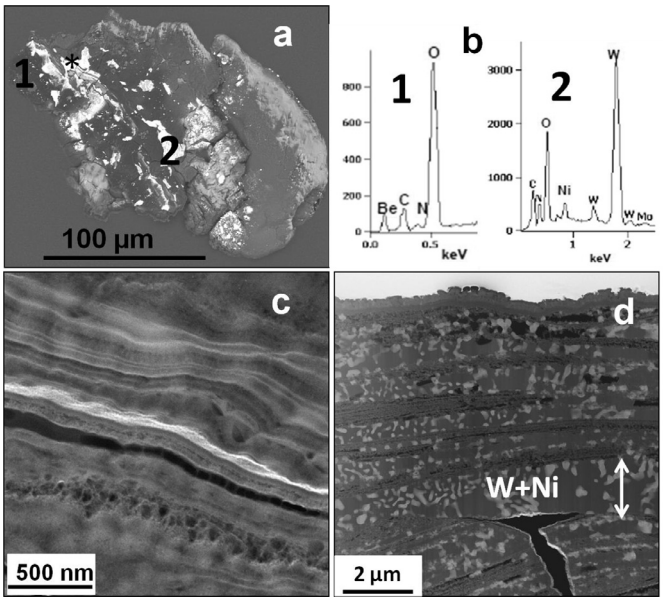


**Fig. 5.** Deposits on apron of Tile 1 after ILW-2 campaign in 2013–2014: (a) a typical agglomerated particle, (b) EDX spectra from two regions, (c) stratified Be-rich deposit, lamella cut from the region indicated as 1; (d) highly porous mixed deposit with light and heavy elements, lamella cut from the region indicated with asterisk. The white double side arrow in Fig. 5d indicate the sublayer rich in W and Ni.

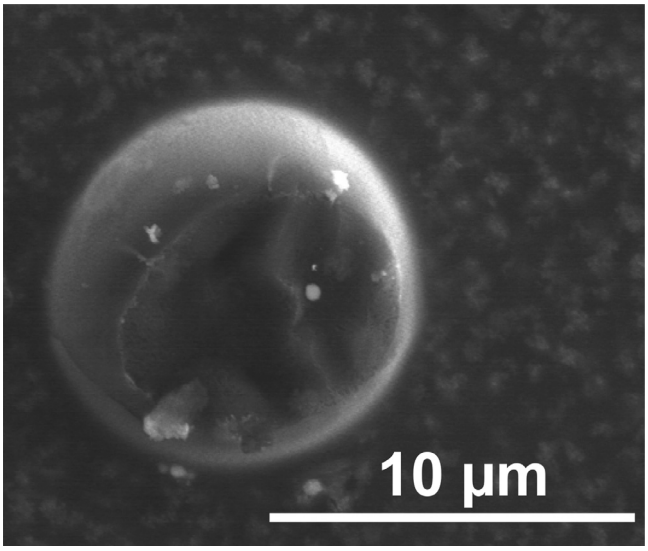


**Fig. 6.** A spherical beryllium particle on apron of Tile 1 after the first ILW campaign, SEM SE mode image.

nitrogen retained after plasma edge cooling by gas injection. The amounts injected in the first and second campaign were respectively $4.84 \times 10^{23}$ and $18.76 \times 10^{23}$ N atoms. In the latter case the nitrogen puffing constituted about 0.9% of the total gas ($D_2$, $H_2$, $N_2$) input. Nitrogen retention in JET co-deposits has already been reported [16,18,20]. Studies dust after the second ILW campaign show that nitrogen is present in all types of re-deposited materials. Corresponding X-ray spectra deposit are in Fig. 5(b).

Rounded beryllium objects, 8–10 µm in diameter and smaller, have been detected on the apron. A small spherical Be droplet shown in Fig. 6 originates most probably from a melt layer on overheated limiters. The volume of a sphere of 10 µm in diameter is $5.25 \times 10^{-10}$ cm$^3$, what corresponds to less than 1 ng in weight and $6.5 \times 10^{13}$ atoms, at atomic density of $1.24 \times 10^{23}$ cm$^{-3}$. In a single sphere there is only a tiny amount of matter. However, from ex-situ analyses it is not possible to conclude on the amount of material ablated when the droplet was passing plasma from the place of origin. Based on the photographic survey, events of limiter melting related to disruptions were not unique and some of them could cause certain material losses. Elongated beryllium splashes (approx. 100 µm in diameter, 5 µm thick, i.e. $1.25 \times 10^{-8}$ cm$^3$) have been found on test mirrors exposed in the main chamber [16].

Matter collected from Tile 3 contains only small carbon-based and ceramic particles. Fairly clean and dust-free tile surfaces could be expected given the fact that the strike point was on that tile during majority of pulses in 2013–2014 [12].

A sloping part of Tile 6 is a deposition zone [12] and this is reflected by character of particles which are similar to what has been detected in the deposition zone of Tile 0 and on the apron of Tile 1, i.e. these are mainly fragments of co-deposits. The detached flakes are relatively large – up to 200 µm in size. They have a layered structure, although granular forms are detected as well. Both composition and internal structure are diversified. The regions rich in either light (Be, C, N, O) and heavy elements are present (W or/and Ni). Although a distinct Be peak was visible only in one spectrum, a high oxygen peak registered in other EDX spectra taken from the areas rich in light elements (C, N) indicates that Be is a major constituent of these particles, because Be is the only species in the light elements mix binding oxygen into a solid compound. For instance, the presence of carbon in the mix has attenuated the low energy (108 eV) X-ray from beryllium (radiation absorption).

Particles/layers rich in tungsten (originating from the W coating) and nickel are detected at the bottom part of particles being small fragments of co-deposit. They have different forms: the smallest objects observed with SEM are fine particles (10–50 nm) embedded in the matrix composed of light elements (Fig. 7) whereas the largest observed pieces are several microns in size.

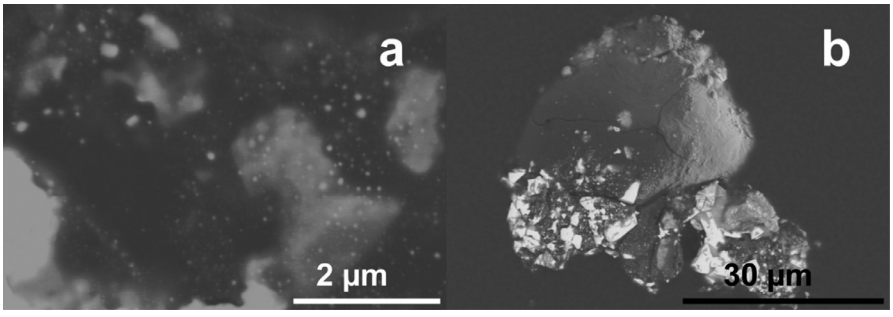


**Fig. 7.** Particles rich in tungsten present in deposits originating from Tile 6, BSE mode.

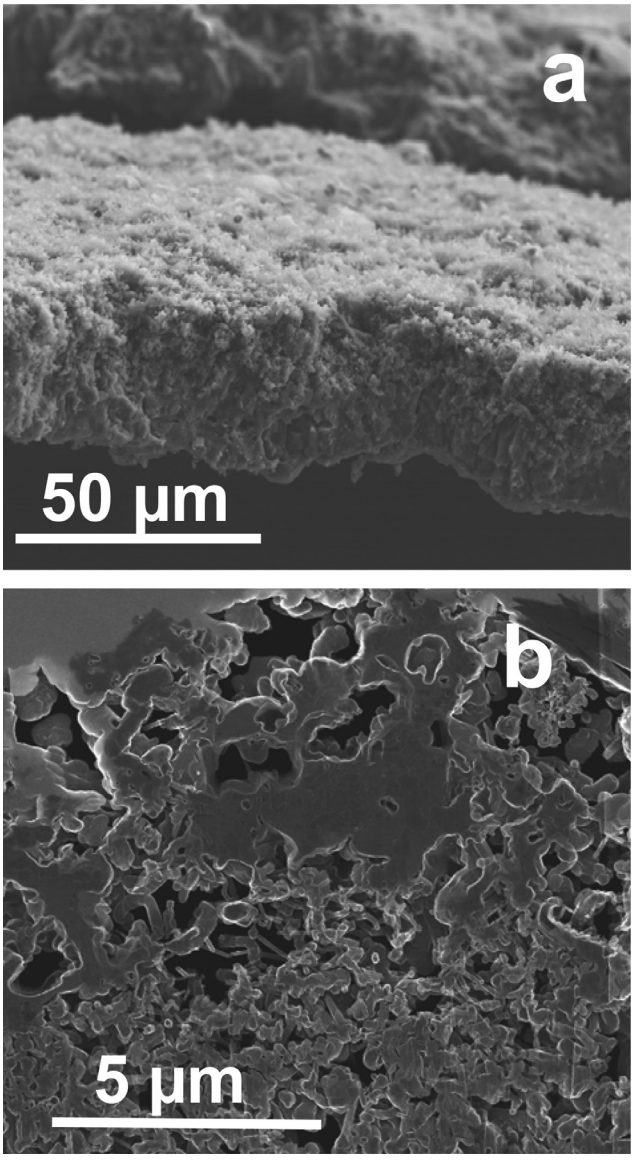


**Fig. 8.** Be-rich co-deposit on the divertor carrier under Tile 6 after ILW-2: a) SEM image of fractured edge, b) STEM image of internal structure.

### 3.2. Dust on the divertor carrier and on test mirrors

Two main groups of particles have been found on the sample collected by brushing the divertor carrier under Tile 6: (i) detached fragments of W-Mo coatings and (ii) beryllium-rich flakes. The size of W or W-Mo debris ranges from several hundred of µm to a few mm. Their surface was overheated, locally revealing melt zones. The largest Be-rich particle was approximately $2 \times 2$ mm in size. Its general appearance and internal structure are presented in Fig. 8(a) and (b), respectively. The surface is uniform: morphology and elemental composition are changed within the individual flake limits. The deposit is composed of fine particles/grains (dimensions from tens of nanometres to two microns), Fig. 8(b), thus making the structure very porous. This form of beryllium deposit has been observed for the first time. Other particles composed of different constituents have been also detected: carbon, ceramics and metals, namely steel, Inconel and copper.

A general appearance and details of a stratified structure deposited on a molybdenum test mirror from the inner divertor are shown in SEM images in Fig. 9(a) and (b), respectively. The layer is smooth, but in several places it is broken most probably due to

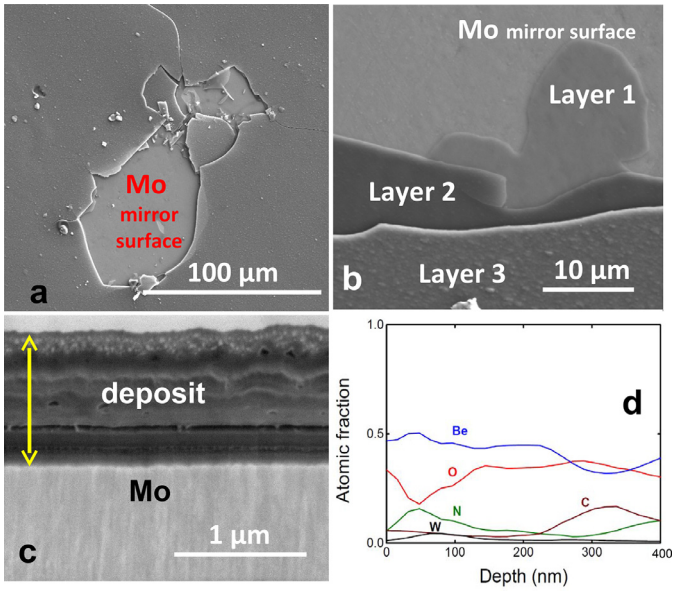


**Fig. 9.** Deposition on a test mirror from the inner divertor after ILW-2: (a) broken dust-forming layer, (b) stratified structure of the broken deposit; (c) deposit cross-section obtained by FIB and (d) ToF-HIERDA depth profiles of elements in the deposit. In Fig. 9c the cross-section through the whole deposit is shown.

internal stresses. As a result, a number of sublayers are displayed. A cross-section obtained by FIB, Fig. 9(c), reveals the layer thickness (1 µm) and an internal structure. It also clearly proves that the deposit adheres poorly to the Mo substrate. Depth profiles obtained by ToF-HIERDA show beryllium as the main constituent of the layers, see Fig. 9(d). A slight increase of the carbon content at the depth of around 300 nm is related to the in-vessel intervention and JET opening in order to retrieve a crashed reciprocating probe. Based on microscopy and HIERDA data one may conclude that the stratified layers were formed in a series of deposition - erosion events in which beryllium, originally transported to the divertor and deposited there, was evaporated and then re-deposited in the shadowed zone of the divertor where mirrors are located. The final composition and structure of the layers are dependent on sticking coefficients of various elements to the substrate. For evaporated Be a sticking coefficient of 0.9 on tungsten surface was determined by Honig [21], but values for a mix of materials containing both low-Z and high-Z elements have not been measured. One may only tentatively expect that they would be in the range 0.9–1.0. The above mentioned processes are to be taken into account in the design of diagnostic systems in a reactor-class machine. It should also be stressed that tungsten and nitrogen are in noticeable amounts especially in the near surface layer (30–70 nm), i.e. the region corresponding to the final period in the campaign. The amount of carbon in the same region is relatively small thus indicating that the operation did not lead to a significant damage of the W coatings despite H-mode discharges.

## 4. Concluding remarks

Examination of dust sampled collected on carbon stickers from various regions of the divertor has identified a range of particles. Besides not ITER-relevant debris from tungsten coatings on CFC tiles there are two major classes of importance to ITER: (i) mixed deposits rich in beryllium and (ii) metal droplets (Be, W, Ni) born in melting events of wall materials. Further split into sub-categories is not intended here for a single reason: the comparison of deposits from the two campaigns clearly proves the increased complexity of particles due to agglomeration of parti-

cles formed originally under different conditions. Therefore, conclusions regarding the size range should be rather restricted to metal droplets and splashes (from 3 µm for droplets to 100 µm for splashes), but certainly not to agglomerates or even co-deposits, which are brittle and easily disintegrate into smaller objects. The collection has proven also that co-deposited layers on the divertor tiles (especially on Tile 0 and apron of Tile 1) adhere well to the substrates. The layers are not peeling-off easily and this explains that the amount of loose matter retrieved after consecutive ILW campaigns did not exceed 2 g.

In summary, tile analyses [12] and locally-specific dust survey have provided very detailed data on the overall morphology of particles. High-resolution dust studies allow, to fair extent, for conclusions on dust generation, its migration and agglomeration. An important contribution of this work to PWI studies in a metal-wall tokamak is a detailed insight into properties of deposits formed on diagnostic components, i.e. mirrors. Transport of light (Be) and heavy (W) metals to the shadowed region in the divertor is well documented once again [20] and it is also shown that such metal layers brake and form dust. In this sense test mirrors serve as long-term deposition monitors. One may consider this type of probes being placed even in a reactor-class machine, especially that the application of removable samples in ITER is under planning [22].

## Acknowledgement

This work has been carried out within the framework of the EUROfusion Consortium and has received funding from the European Union's Horizon 2020 research and innovation programme under grant agreement number 633053. The views and opinions expressed herein do not necessarily reflect those of the European Commission.

## References

[1] B. Braams, Characterisation of size, composition and origins of dust in fusion devices, IAEA (2012) http://www-nds.iaea.org/reports-new/indc-reports.
[2] D. Ivanova, et al., Survey of dust formed in the TEXTOR tokamak: structure and fuel retention, Phys. Scr. T138 (2009) 014025.
[3] E. Fortuna-Zalesna, et al., Dust survey following the final shutdown of TEXTOR: metal particles and fuel retention, Phys. Scr. T167 (2016) 014059.
[4] B. Pegourie, et al., Deuterium inventory in Tore Supra: coupled carbon–deuterium balance, J. Nucl. Mater. 438 (2013) S120.
[5] E. Fortuna-Zalesna, et al., Characterization of dust collected after plasma operation of all-tungsten ASDEX Upgrade, Phys. Scr. T159 (2014) 014066.
[6] M. Balden, et al., Comparison of chemical composition and morphology of dust particles from various fusion devices, in: Proc. PFMC-15, A-016/P-12, Aix-en-Provence, France, 2015.
[7] M. De Angeli, et al., Dust characterization in FTU tokamak, J. Nucl. Mater. 463 (2015) 847.
[8] G.F. Matthews, et al., JET ITER-like wall – overview and experimental programme, Phys. Scr. T145 (2011) 014001.
[9] S. Brezinsek, et al., Beryllium migration in JET with ITER-like wall plasmas, Nucl. Fusion 55 (2015) 063021.
[10] M. Rubel, et al., Overview of erosion–deposition diagnostic tools for the ITER–Like Wall in the JET tokamak, J. Nucl. Mater. 438 (2013) S1204.
[11] A. Widdowson, et al., Material migration patterns and overview of first surface analysis of the JET ITER-Like Wall, Phys. Scr. T159 (2014) 014010.
[12] A. Widdowson et al., Overview of the JET ITER-Like Wall divertor, These proceedings.
[13] J. Likonen, et al., Measurement of dust conversion factor for the JET carbon divertor Phases, J. Nucl. Mater. 463 (2015) 842.
[14] A. Baron–Wiechec, et al., First dust study in JET with the ITER-Like Wall: sampling, analysis and classification, Nucl. Fusion 55 (2015) 113033.
[15] M. Rubel, et al., Mirror test for international thermonuclear experimental reactor at the JET tokamak: an overview of the program, Rev. Sci. Instr. 77 (2006) 063501.
[16] A. Garcia-Carrasco et al., *Modification of diagnostic mirrors in JET*, These proceedings.
[17] J. Likonen, et al., First results and surface analysis strategy for plasma-facing components after JET operation with the ITER-Like Wall, Phys. Scr. T159 (2014) 014016.
[18] P. Petersson, et al., Co-deposited layers in the divertor region of JET-ILW, J. Nucl. Mater. 463 (2015) 814.
[19] M. Mayer, et al., Erosion and deposition in the JET divertor during the first ILW campaign, Phys. Scr. T167 (2016) 014051.
[20] D. Ivanova, et al., An overview of the comprehensive first mirror test in JET with ITER-Like Wall, Phys. Scr. T159 (2014) 014011.
[21] R.E. Honig, Pressure data for the more common elements, RCA Rev. 18 (1957) 195.
[22] Ph. Mertens, et al., Removable samples for ITER – a feasibility and conceptual study, Phys. Scr. T159 (2014) 014004.